SmallSat Solar Axion X-ray Imager (*SSAXI*)

Jaesub Hong
Harvard University
Cambridge, MA 02138; 617-496-7512
jhong@cfa.harvard.edu

Suzanne Romaine, Christopher S. Moore, Katharine Reeves, Almus Kenter
Smithsonian Astrophysical Observatory
Cambridge, MA 02138; 617-496-7719
sromaine@cfa.harvard.edu

Brian D. Ramsey, Kiranmayee Kilrau
NASA Marshall Space Flight Center
Huntsville, AL 35812; 256-961-7784
Brian.Ramsey@nasa.gov

Kerstin Perez
Massachusetts Institute of Technology
Cambridge, MA 02139; 617-324-1522
kmperez@mit.edu

Julia Vogel, Jaime Ruz Armendariz
Lawrence Livermore National Laboratory
Livermore, CA 94550; 925-424-4815
Vogel9@llnl.gov

Hugh Hudson
Space Science Laboratory
UC Berkeley, CA 94720; 510-643-0333
hhudson@ssl.berkeley.edu

ABSTRACT

The axion is a promising dark matter candidate as well as a solution to the strong charge-parity (CP) problem in quantum chromodynamics (QCD). Therefore, discovery of axions will have far-reaching consequences in astrophysics, cosmology and particle physics. We describe a new concept for SmallSat Solar Axion X-ray Telescope (*SSAXI*) to search for solar axions or axion-like particles (ALPs). Axions or ALPs are expected to emerge abundantly from the core of stars like the Sun. *SSAXI* employs Miniature lightweight Wolter-I focusing X-ray optics (MiXO) and monolithic CMOS X-ray sensors to form a sensitive X-ray imaging spectrometer in a compact package (~10 x 10 x 60 cm). The wide energy range (~0.5 – 5 keV) of *SSAXI* is suitable for capturing the prime spectral feature of axion-converted X-rays (peaking at ~3 – 4 keV) from solar X-ray spectra. The high angular resolution (~30 arcsec) and large field of view (~40 arcmin) in *SSAXI* will easily resolve the enhanced X-ray flux over the 3 arcmin wide solar core while fully covering the X-ray activity over the entire solar disc.

INTRODUCTION

Modern cosmology firmly establishes that dark matter makes up 27% of the total energy budget or 85% of the total matter in the Universe.[1] In spite of its abundance, the nature of dark matter remains one of the fundamental mysteries in astrophysics and cosmology and cannot be explained within the otherwise very successful Standard Model of particle physics. Currently the leading candidates for dark matter are Weakly Interacting Massive Particles (WIMPs), axions and sterile neutrinos.

Originally postulated by Peccei and Quinn, the axion is a hypothetical elementary particle arising from the most viable solution for the strong charge-parity (CP) problem in quantum chromodynamics (QCD).[2] Since standard axions of a symmetry-breaking scale (of the

order of the electroweak interaction) were ruled out[3,4], newer models of arbitrary scales were developed by Kim-Shifman-Vainshtein-Zakharov (KSVZ)[5,6] and Dine-Fischler-Srednicki-Zhitnitskii (DFSZ).[7,8] These lighter axions, and the more general ALPs, which are well motivated by string theory, are postulated to interact so weakly that they are called "invisible". Nevertheless, these theoretically inspired axions or ALPs would have far-reaching consequences in astrophysics and cosmology. For instance, ALPs, which are expected to be generated in the hot thermal plasma of stellar cores, provide a new process of energy loss in stellar evolution.[9] ALPs are also proposed as a solution to the apparent transparency of the Universe to very high energy TeV gamma-rays.[10] It has been suggested that efficient conversion of photons to ALPs expected in the high magnetic field of atmospheres of compact objects such as magnetars can lead to distinct spectral absorption signatures.[11] Alternatively, axions could be generated within neutron stars by nucleon-nucleon bremsstrahlung, and spectral signatures from their decay into gamma-rays can be used to constrain the axion mass.[12]

According to inflation theory, primordial axions of low kinetic energy should have been created abundantly.[13] These primordial axions of low mass (< ~1 meV) are a particularly attractive candidate for dark matter because many would have survived and filled the universe because of their lack of a decay process into lighter particles.[14]

Given the fact that the axion is a promising candidate for dark matter and a solution for the strong CP problem in QCD along with its numerous implications in astrophysics, many experimental techniques have been developed over the years for the search for axions or ALPs. These techniques include solar axion searches using 'helioscopes' (e.g., *CAST*, *IAXO*), polarization changes of light propagation in the magnetic field (e.g., *PVLAS*), light shining through barriers (e.g., *ALPS*-I, II), resonance effects in Josephson junctions (e.g., *ORGAN*), electron recoils in cryogenic detectors (e.g., *CDMS*).

We introduce a new mission concept, SmallSat Solar Axion X-ray Imager (*SSAXI*) that is designed to search for axions or ALPs emerging from the solar core by capturing axion or ALP-converted X-rays in the solar magnetic field and thus effectively imaging the solar core.

MOTIVATION AND OBJECTIVES

Axion emerging from the Solar Core

Among many experimental techniques that have been developed over the years for the search of axions, solar axions are a primary target for many axion hunters. ALPs are expected to emerge abundantly from the hot plasma in the stellar core through the incoherent Primakoff effect, where a photon converts into an axion in the electric field of a charged particle. The emerging axions have a blackbody distribution of the thermal conditions in the solar interior with the peak and mean energies of roughly 3 and 4 keV, respectively. Almost all of axion search methods rely on the inverse coherent Primakoff effect, where an ALP, otherwise invisible, is re-converted to an X-ray photon by transverse magnetic fields. In the case of solar axions, this conversion can occur in the magnetic fields in the solar atmosphere, or laboratory magnetic fields.

Fig. 1A compares the solar X-ray spectra during a quiet sun state (A4: ~4 ×10^{-8} W m^{-2}) and a "deep solar minimum" state (<A1: ~7×10^{-10} W m^{-2}) with the

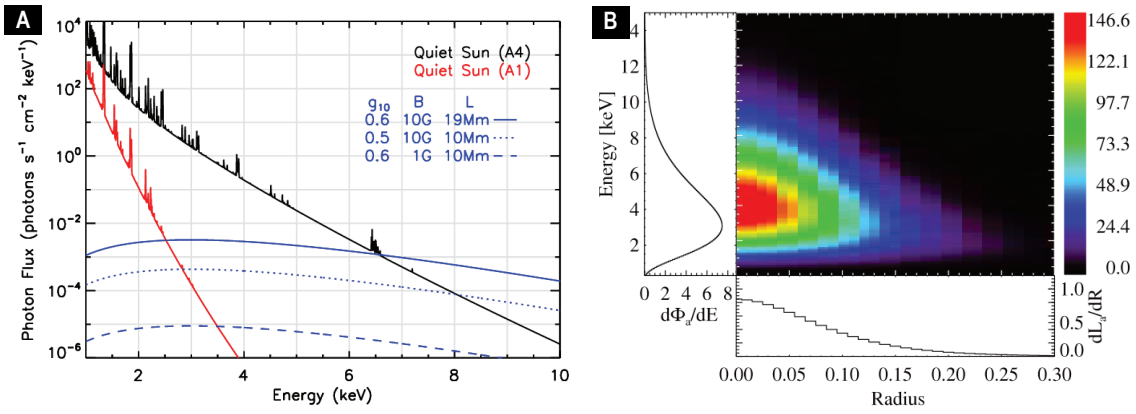

Fig. 1 (A) Solar X-ray fluxes during two quiet sun states (black & red; scaled for a 0.1 $R_\odot$ disc region)[15] in comparison with the expected axion-converted X-ray signal (blue) from the central 0.1 $R_\odot$ disc.[16] **(B)** Solar axion surface luminosity depending on energy and relative solar radius.[16] About 80% and 50% of the axion-covered X-ray fluxes are from the central 0.2 and 0.1 $R_\odot$ disc, respectively.

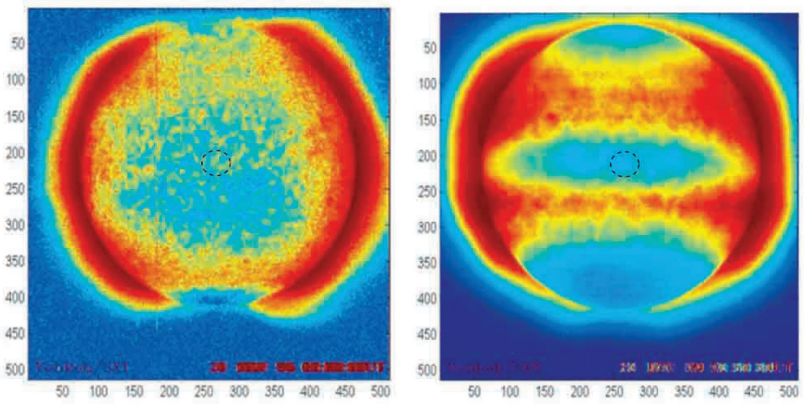

Fig. 2 Solar images of 250 eV to a few keV from *Yohkoh* (1991 – 2001): (***Left***) a composite image of the solar minimum in 1996 (***Right***) a composite image of during solar maximum. The circles indicate the region of expected X-ray brightening spot at the center,[9] while neither image shows an enhancement at disk center, but these data are not at all optimal.

expected axion-converted X-ray fluxes from the central 0.1 $R_\odot$ disc (~50% of the total). The latter is proportional to g^4 $(B\ L)^2$ where g, B and L is the axion-photon coupling constant, the magnetic field strength and conversion length, respectively. Given the size of the solar core and the expected axion-converted X-ray spectra, *the axion or ALP-induced X-ray signature can be determined decisively when it is simultaneously spatially resolved and spectrally detected* with a sensitive soft X-ray imaging spectrometer (**Fig. 1B**), whereas the imaging or spectral signature alone is difficult to detect or allow other interpretations.

Fig. 2 shows the combined solar images in a soft X-ray band during the solar minimum in 1996 and the solar maximum in 2001 taken with *Yohkoh*. The black circles at the center are the region of the expected enhancement in the X-ray flux from axion or ALP conversion.[9] Both images show no enhancement at the center, and instead exhibit strong brightening at the rim of the solar disc while high X-ray activities are observed over a wide band near ±35° in latitude during the solar maximum.

Fig. 3 compares the exclusion region in the coupling (g) versus axion mass space set by leading axion search experiments with the prospects of upcoming *NuSTAR* observations and the proposed concept *SSAXI*. Even with a relatively small effective area (>~2 cm^2), a dedicated 1 yr observation with *SSAXI* can outperform a few 100 ks *NuSTAR* observations by a factor of ~10 in terms of axion signal detection (~80% lower limit for g) due to a lower background in *SSAXI* (<~0.01×). The fast readout system of the *SSAXI* focal plane also enables effective observations for a wider range of solar states, whereas *NuSTAR* axion search is somewhat limited to sub-A solar states.

Sterile Neutrino

The design of the *SSAXI* concept can be also optimized for search of the keV-scale sterile neutrino, another promising candidate for dark matter. Motivated by neutrino mass and oscillation measurements, sterile neutrino dark matter would decay via neutrino mixing into a photon and an active neutrino, producing a mono-energetic photon signature at $E = m_s/2$. Astrophysical X-ray observations have produced the most stringent constraints on sterile neutrino decay across a wide mass range,[17] with other significant constraints from structure formation.[18] In recent years, an exciting, but controversial, signal of sterile neutrino decay has been reported at $E \sim 3.5$ keV. This signal has been independently observed in stacked X-ray clusters, the Perseus Cluster, Andromeda, the Galactic Center, and the Galactic halo.[19,20] If confirmed, such a discovery would be revolutionary for the fields of particle physics, astrophysics, and cosmology. However, initial analysis with the brief *Hitomi* dataset disputes this

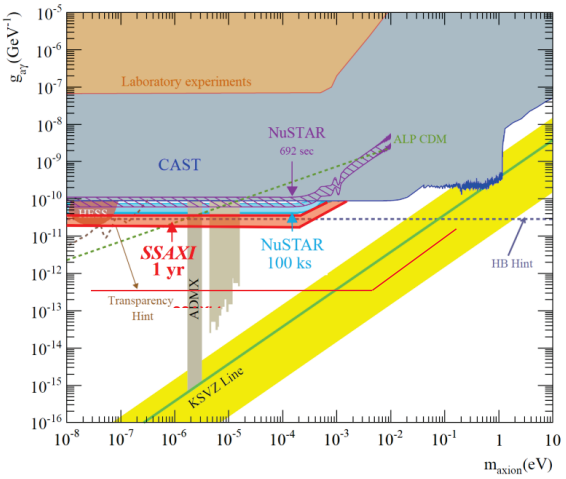

Fig. 3 Exclusion region in the axion-photon coupling ($g_{a\gamma}$) versus the axion rest mass (m_a) set by various experiments overlaid with the expected performance (preliminary) of a 100 ks *NuSTAR* observation (cyan; 75% dead time) and a 1yr *SSAXI* observation (12U CubeSat version) near a solar minimum (red; 70% duty cycle).

claim. The recent constraints on sterile neutrino decay set by the *NuSTAR* observations of the Galactic center[17] were utilizing only zero-bounce photons, collected by ~ 5 – 10 cm^2 effective area. This shows that a dedicated continuous observation with a compact telescope of a moderate effective area would make significant improvement; the X-ray energy resolution (<~150 eV) in the range 3 – 4 keV, which the *SSAXI* concept would provide, is sufficient to resolve this controversy.

INSTRUMENT DESIGN

Fig. 4 illustrates a 12U CubeSat version of the *SSAXI* spacecraft (S/C) with the main instrument, an X-ray Imaging Spectrometer (XIS). The XIS is a compact focusing X-ray telescope in a small form factor (~10 × 10 × 60 cm, ~6U), weighing about 5 kg. It consists of Miniature Wolter-I X-ray Optics (MiXO) and a CMOS X-ray Active Pixel Sensor (APS). MiXO, configured for a focal length of 50 cm, provides a wide field of view (~40 arcmin dia.) with a high angular resolution (~30 – 60 arcsec) over the 0.5 – 5 keV band. The CMOS X-ray sensor covers the same band with a good energy resolution (<150 eV at 2 keV). A thick optical blocking filter attenuates high solar soft X-ray flux (<1.5 keV) while allowing >~50% of hard X-ray flux (>~3 keV) for efficient detection of axion-converted hard X-rays.

Table 1 summarizes key parameters of the *SSAXI* XIS for two possible configurations. A SmallSat S/C with a larger payload capability can accommodate multiple units of the XIS with a longer focal length. For instance, the MicroSat S/C developed by Blue Canyon Technologies (BCT) allows a payload volume and mass of ~45 × 45 × 80 cm and ~50 kg, respectively, and it can easily carry 3 XIS of 70 cm focal length. The 3 XIS can have different X-ray filters to optimize their sensitivity to different solar flare states and the energy band pass to cover a wide range of solar states.

Table 1 Key Parameters of the *SSAXI* XIS for two S/C configurations

Parameters	12U (1 x 2 x 6U)	SmallSats
Focal length	50 cm	70 cm
No. of shells	10+	10+
Shell size (dia.)	4 – 7 cm	9 – 10 cm
Mass (kg)	5	6
Detector (cm^2)	1.6 × 1.6	1.6 × 1.6
FoV (Dia.)	~35 arcmin	
Angular resolution	~30 – 50 arcsec (on / off-axis)	
Effective area (A_E, cm^2)	1 @ 3 keV	2 @ 3 keV
Grazing angles	0.57°– 0.93°	0.71°– 0.86°

Miniature X-ray Optics

Modern X-ray astronomy missions utilize grazing-incidence optics with Wolter-I geometries,[14] which combines reflections from a parabolic and a hyperbolic surface of a barrel shaped mirror to reduce off-axis aberrations (over a single bounce system) for imaging. To increase the collecting area of these telescopes, several barrel shaped mirrors of varying diameter can be nested one inside the other along the same optical axis. While the conventional X-ray telescopes such as *Chandra X-ray Observatory* and *XMM-Newton* consists of very large X-ray optics with 7 – 10 m focal length, the advances in the X-ray optics technology over the years now enables a compact, yet powerful X-ray optic.

SSAXI employs Miniature X-ray Optics (MiXO), compact lightweight Wolter-I X-ray optics for CubeSat/SmallSat missions. MiXO leverages the recent and on-going development to build lightweight Wolter-I X-ray optics based on the electroformed Ni-alloy replication (ENR) technique.[21,22] In ENR, NiCo shells are electroformed from a precision machined mandrel

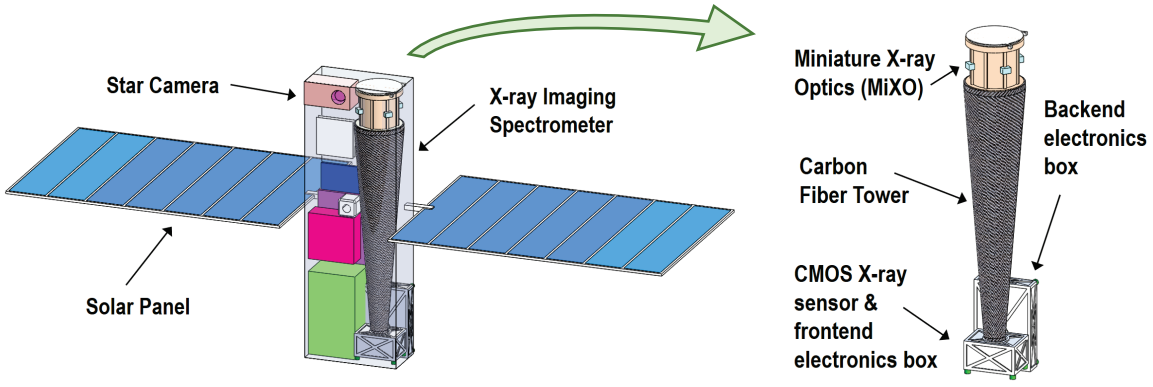

Fig. 4 (*left*) SmallSat Solar Axion X-ray Imager (*SSAXI*) spacecraft with an X-ray Imaging Spectrometer (XIS), weighing 11 kg in a 20 x 10 x 60 cm form factor (~12U). **(*right*)** Main subsystems of the XIS.

and released through a thermal cycle (chilled water). The surface quality of the shells is determined by the mandrel surface and the figure of the shells is determined by the mandrel figure coupled with the stress during the release process.

Fig. 5 illustrates the design concept for MiXO on *SSAXI*, where the optics consist of ten 250 µm thick NiCo shells in an optics housing and "spider" support structure. The overall structure including the housing fits inside of a 1U volume with ~10 cm dia. × 9 cm length (**Fig. 5A**). Each shell has slightly different length depending on the shell radius, a.k.a. a butterfly design, to allow a wide field of view (FoV~40 arcmin dia.) with high angular resolution (**Fig. 5B**).

The configuration should enable ~ 2 cm^2 on-axis effective area in the 3 – 4 keV band within 30 – 40 arcsec HPD after a thick optical blocking filter (roughly equivalent to a ~250 µm thick Be window). The thick filter is required to suppress soft X-rays below 1 – 1.5 keV, which otherwise dominate the X-ray flux and cause pile-ups on the CMOS X-ray sensors.

CMOS X-ray Sensors

Fig. 6 shows the focal plane design of the *SSAXI* XIS, which consists of the frontend and backend electronics boxes. The *SSAXI* XIS focal plane is based on a monolithic CMOS X-ray APS, which is known as "Big Minimal III" (BM-III). CMOS X-ray sensors are becoming the next state-of-art detectors for X-ray telescopes, just as CMOS optical sensors like devices in SoloHi and WISPR are replacing CCD imagers.[23] The BM-III devices were designed by SRI/Sarnoff and share a common heritage with the flight CMOS imagers provided by SRI for other programs.[24,25]

The back-illuminated BM III devices with 10 – 20 µm thick Si absorber have sufficient QE over the 0.5 – 7 keV band that can separate the axion or ALP-converted X-rays peaking at 3 – 4 keV from the soft solar X-ray spectra. The fast readout in the BM-III devices enables high spectral resolution at high temperature. *Forgiving thermal requirements are suitable for resource-limited SmallSats.* It also enables a wide dynamic range without pile-ups, which is essential for observing highly variable solar X-ray activities. Small pixel size (~6 arcsec per pixel for a focal length of 50 cm) is sufficient to oversample the MiXO point spread function (PSF ~30 arcsec HPD at on-axis). Each pixel has its own electronics channel (i.e., Active Pixel Sensor), eliminating the need for long charge transfers, and making the device inherently radiation tolerant (>100 krads), which is ideal for space applications.

Each BM-III device has a 1k × 1k array of 16 µm 6-Transistor Pinned Photo Diode (6T PPD) pixels. The BM-III 1k × 1k array consists of two 512 columns × 1k row halves. Each half has its own 512 column-at-a-time, clamp-and-sample analog Correlated Double Sampling (CDS) processor. Each 512-column processor then reduces to a single buffered output via a 512:1 multiplexer. The maximum possible rate from each output is ~20 MHz (per pixel). The maximum possible read rate of a full frame, with two output channels operating, is therefore 40 Hz (per frame). For the *SSAXI* focal plane, the full FoV (~40 arcmin dia.) is covered by ~400 × 400 pixels, less than a quarter of the pixel array. Therefore, one 512-column processor is sufficient, and only the illuminated pixels/rows need to be read out, greatly reducing the amount of telemetered data, and potentially reducing the required speed of the associated electronics.

Onboard Data Processing Scheme

A main challenge for *SSAXI* is onboard data processing under the large solar X-ray flux. For a 12U CubeSat version with ~2 cm^2 effective area at 1 keV, the full downlink of observed X-ray event lists may be too large even during quiet solar states (A: ~10^{-8} W m^{-2}). In

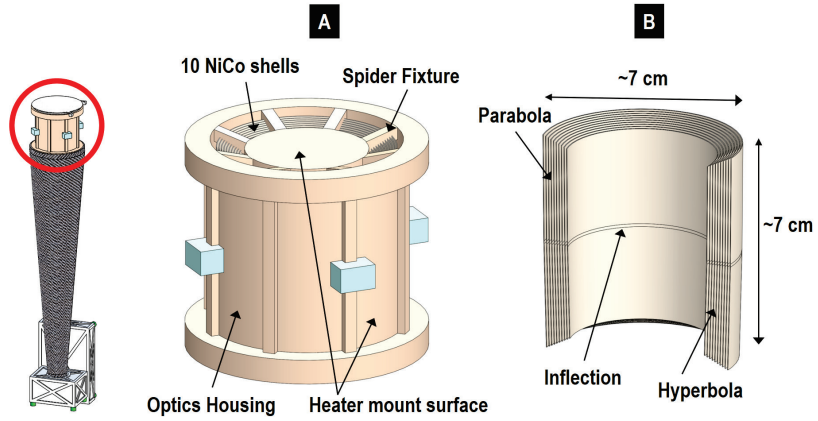

Fig. 5 MiXO on *SSAXI*. **(A)** Optics housing and support structure **(B)** Cut-away view of 10 NiCo shells in a butterfly (variable shell lengths) design to ensure a wide field coverage (~40 arcmin dia.).

order to enable efficient search for X-ray signature of solar axions under the large X-ray flux from the solar disc experiencing regional variations (e.g., micro- and nano-flares), the data will be telemetered in two modes – event and spectral modes with the latter being the main telemetry mode.

Table 2 summarizes the expected data rate of *SSAXI* during the solar minimum. In the event mode, energies of all 3×3 pixels surrounding each trigger pixel are telemetered. The data rate of the full event mode data is expected to be over multi GBytes per day (e.g., ~10 GBytes per day for 1 kcps), so a small subset (e.g., about 10 mins worth) will be downloaded daily for diagnostic and parameter optimization purpose (e.g., event and charge split threshold, etc.).

For search of X-ray signature of solar axions, the spectral mode is utilized. Since the X-ray signature of solar axions is expected to be more clearly identifiable if both the spatial (i.e., an excess in the solar core over the solar disc) and spectral (i.e., an excess in the 3 – 4 keV band over the broadband) signatures are observed, we first divide the solar disc into about 5000 spatial resolution units (~30–60 arcsec or 5–10 pixel dia. per unit). Then, we accumulate the daily X-ray spectrum of each spatial unit. Based on the activity level of each spatial unit, we accumulate a set of spectra while bookkeeping the matching exposure interval of each level. For instance, four sets of the spectra can be accumulated, corresponding to the solar state levels of sub-A (< ~10^{-8} W m^{-2}), A (~10^{-8} – 10^{-7} W m^{-2}), B (~10^{-7} – 10^{-6} W m^{-2}), and above B (> ~10^{-6} W m^{-2}). The on-board process can tally on-going average X-ray counts of each spatial unit over a fixed interval (e.g., 10 min), and the average X-ray count level will determine which level of the spectra will be accumulated from the previous interval. In this way, the low state spectral set will provide the quietist state of the solar spectra over the entire disc in ~30 – 60 sec resolutions, providing the highest chance of detecting X-ray signature of solar axions.

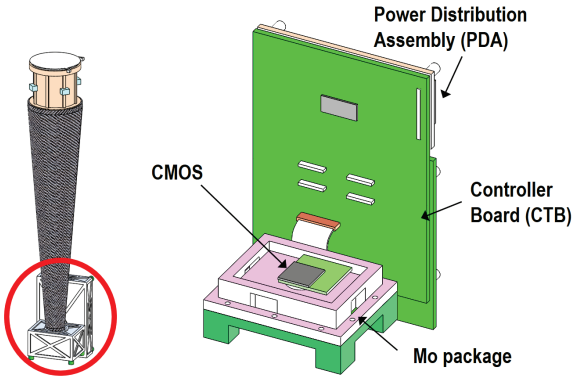

Fig. 6 Focal plane design of the *SSAXI* XIS. The CMOS Imager Headerboard is located below Mo package.

To keep the pile-ups below 1%, the average incident X-rays on the active region of the detector should be limited to about 25 kcps (or 0.2 cps per pixel at 20 Hz readout). A ~250 µm Be window will allow about 1 kcps of solar X-rays incident on the CMOS X-ray sensor at solar A states. The daily 4 × 5k spectra of 20 eV bins over 0.5 – 10 keV would be about 20 MB/day, while the event data of 25 kcps would be about 25 GB/day. The latter can be prohibitively high for SmallSats, as aforementioned. Thus, with a small portion of events for daily diagnostics, the expected total data rate of the spectral mode data for 1 yr science operation is about 14 GB /yr with 70% duty cycle and 20% overhead for HK and data headers (**Table 2**).

Table 2 Data Rate of *SSAXI* XIS

Parameter	**Values**	
Readout freq.	20 Hz	
Pile-up limit	<1 %	
Max event rate	25 kcps over ~360 x 360 pixels	
Dynamic range	A states with 250 µm Be window	
Duty cycle	50%	
Mode	**Event**	**Spectral**
Data type	3×3 pixel energies of each event	3×5k spectra, 512 bins with 20 eV steps
Daily duration	10 min	16 hr
Software filter	< 1 kcps	None
Daily rate	4 MB	20 MB
Total data rate	14 GB for 1 yr science op	

MISSION DESIGN

Mission Implementation

SSAXI can be designed to be a secondary mission to have a rideshare to a sun-synchronous orbit at an altitude somewhere between 600 and 1000 km. Alternatively, it can have a rideshare to a LEO or be released to a LEO from the International Space Station. Sun-synchronous orbits enables uninterrupted continuous observations of the Sun with the XIS in a more stable thermal environment. On the other hand, they are nearly polar orbits, where the instrument can experience higher instrumental background than in LEOs of low inclinations that avoid the South Atlantic Anomaly (SAA). The low inclination orbits, however, can reduce the observing time by more than half due to Earth occultations, which will also force the XIS to

experience the periodic changes in its thermal environment, thus requiring a more careful design of the thermal system (e.g., *NuSTAR* observations of the Sun). For search of sterile neutrino, LEOs would be preferable. More in-depth simulations will be required to assess upsides and downsides of each orbital configuration.

Given expected relatively low costs of CubeSat/SmallSat missions, multiple *SSAXI* missions can be deployed to various orbital configurations, depending on launch opportunities, to establish higher photon statistics, which in turn enhances a chance of detecting X-ray signature of solar axions or provides a stronger constraint on the axion coupling constant.

SUMMARY

SSAXI is a SmallSat concept designed to search for X-ray signature of solar axions by capturing X-rays converted from solar axions or ALPs through inverse Primakoff effects. Since the solar core is expected to generate axions or ALPs whose energy peaks at 3 – 4 keV, the converted X-rays will have the spectrum peaking in the similar energy band, and this spectral signature is expected to be more prominent along the line of sight to the solar core. The imaging spectroscopy of the solar disc, therefore, enables unambiguous identification of the X-ray signature of solar axions.

Recent advances in X-ray telescopes and instruments such as Miniature X-ray Optics (MiXO) and monolithic CMOS X-ray sensors enable a compact X-ray imaging spectrometer suitable for CubeSat/SmallSat missions.

References

1. Planck Collaboration (2015). “Planck 2015 Results XIII. Cosmological parameters”. Astronomy & Astrophysics, 594 (13): 63.
2. Peccei, R. D. & Quinn, H. R. (1977). "CP Conservation in the Presence of Pseudoparticles". *Physical Review Letters*. 38 (25): 1440–1443.
3. Weinberg, Steven (1978). "A New Light Boson?". *Physical Review Letters*. 40 (4): 223–226.
4. Wilczek, Frank (1978). "Problem of Strong P and T Invariance in the Presence of Instantons". *Physical Review Letters*. 40 (5): 279–282.
5. Kim, J.E. (1979). "Weak-Interaction Singlet and Strong CP Invariance". *Phys. Rev. Lett*. 43 (2): 103–107.
6. Shifman, M.; Vainshtein, A.; Zakharov, V. (1980). "Can confinement ensure natural CP invariance of strong interactions?". *Nucl. Phys*. B166 (3): 493–506.
7. Dine, M.; Fischler, W.; Srednicki, M. (1981). "A simple solution to the strong CP problem with a harmless axion". *Phys. Lett.* B104 (3): 199–202.
8. Zhitnitsky, A. (1980). "On possible suppression of the axion-hadron interactions". *Sov. J. Nucl. Phys.* 31: 260.
9. Carlson, E. D., & Li-Sheng, T. (1996), “Pseudoscalar conversion and X-rays from the sun”, *Physics Letters B*, 365, 193
10. De Angelis, A.; Mansutti, O.; Roncadelli, M. (2007). "Evidence for a new light spin-zero boson from cosmological gamma-ray propagation?". *Physical Review D.* 76 (12): 121301.
11. De Angelis, A.; Mansutti, O.; Persic, M.; Roncadelli, M. (2009). "Photon propagation and the very high energy gamma-ray spectra of blazars: How transparent is the Universe?". *Monthly Notices of the Royal Astronomical Society: Letters.* 394: L21–L25.
12. Berenji, B.; Gaskins, J.; Meyer, M. (2016). "Constraints on axions and axionlike particles from Fermi Large Area Telescope observations of neutron stars". *Physical Review D.* 93 (14): 045019.
13. Redondo, J.; Raffelt, G.; Viaux Maira, N. (2012). "Journey at the axion meV mass frontier". *Journal of Physics: Conference Series.* 375 022004 (2): 022004.
14. Sikivie, P. (2009). “Dark matter axions”. Invited talk at the Workshop *Crossing the Boundaries: Gauge Dynamics at Strong Coupling* (arXiv:0909.0949)
15. Brooks, D. H., Warren, H. P., Williams, D. R., & Watanabe, T. (2009), “Hinode/Extreme-Ultraviolet Imaging Spectrometer Observations of the Temperature Structure of the Quiet Corona”, *Astrophysical Journal* 705, 1522.
16. Zioutas, K., Tsagri, M., Semertzidis, Y., et al. (2009), “Axion searches with helioscopes and astrophysical signatures for axion(-like) particles”, *New Journal of Physics*, 11, 105020
17. Perez, K., Ng, K. C. Y., Beacom, J. F., et al. (2017), “Almost closing the ν MSM sterile neutrino dark matter window with NuSTAR”, *Physical Review D* 95, 123002
18. Cherry, J. F., & Horiuchi, S. (2017), “Closing in on resonantly produced sterile neutrino dark matter”, *Physical Review D* 95, 083015

19. Bulbul, E., Markevitch, M., Foster, A., et al. (2014), "Detection of an Unidentified Emission Line in the Stacked X-Ray Spectrum of Galaxy Clusters", *Astrophysical Journal* 789, 13

20. Boyarsky, A., Ruchayskiy, O., Iakubovskyi, D., & Franse, J. (2014), "Unidentified Line in X-Ray Spectra of the Andromeda Galaxy and Perseus Galaxy Cluster", *Physical Review Letters* 113, 251301

21. Romaine, S., Basso, S., Bruni, R. J., Burkert, W., Citterio, O., Conti, G., Engelhaupt, D., Freyberg, M. J., Ghigo, M. & Gorenstein, P. (2006) "Development of a prototype nickel optic for the Constellation-X hard x-ray telescope: IV", *SPIE* 6266E..39R

22. Hong, J., & Romaine, S. (2016). "Miniature lightweight X-ray optics (MiXO) for surface elemental composition mapping of asteroids and comets". *Earth, Planets and Space*, 68(1), 35.

23. Korendyke, C. M., Vourlidas, A., Plunkett, S. P., et al. (2013), "Development and test of an active pixel sensor detector for heliospheric imager on solar orbiter and solar probe plus", *Proceedings of the SPIE*, 8862, 88620J

24. Janesick, J., Pinter, J., Potter, R., Elliott, T., Andrews, J., Tower, J., Cheng, J., & Bishop, J. (2009, August). "Fundamental performance differences between CMOS and CCD imagers: part III". In *Society of Photo-Optical Instrumentation Engineers (SPIE) Conference Series*, 7439.

25. Janesick, J., Pinter, J., Potter, R., Elliott, T., Andrews, J., Tower, J., Grygon, M., & Keller, D. (2010, July). "Fundamental performance differences between CMOS and CCD imagers: part IV". In *Society of Photo-Optical Instrumentation Engineers (SPIE) Conference Series*, 7742.